High- and Low-Mobility Stages in the Synaptic Vesicle Cycle

Dirk Kamin,[†△] Marcel A. Lauterbach,[‡△] Volker Westphal,[‡] Jan Keller,[‡] Andreas Schönle,[‡] Stefan W. Hell,[‡] and Silvio O. Rizzoli[†*]

[†]STED Microscopy of Synaptic Function, European Neuroscience Institute, and [‡]Department of NanoBiophotonics, Max Planck Institute for Biophysical Chemistry, Göttingen, Germany

ABSTRACT   Synaptic vesicles need to be mobile to reach their release sites during synaptic activity. We investigated vesicle mobility throughout the synaptic vesicle cycle using both conventional and subdiffraction-resolution stimulated emission depletion fluorescence microscopy. Vesicle tracking revealed that recently endocytosed synaptic vesicles are highly mobile for a substantial time period after endocytosis. They later undergo a maturation process and integrate into vesicle clusters where they exhibit little mobility. Despite the differences in mobility, both recently endocytosed and mature vesicles are exchanged between synapses. Electrical stimulation does not seem to affect the mobility of the two types of vesicles. After exocytosis, the vesicle material is mobile in the plasma membrane, although the movement appears to be somewhat limited. Increasing the proportion of fused vesicles (by stimulating exocytosis while simultaneously blocking endocytosis) leads to substantially higher mobility. We conclude that both high- and low-mobility states are characteristic of synaptic vesicle movement.

INTRODUCTION

The major principles of synaptic vesicle function have been established by more than five decades of synaptic research. Synaptic vesicles fuse at active zones, thereby releasing their neurotransmitter onto postsynaptic receptors, and are subsequently endocytosed and refilled with neurotransmitter (in what constitutes synaptic vesicle recycling (1)). Although the processes of exo- and endocytosis have been described in molecular detail, the general mobility of the vesicles is less well understood.

The current view of synaptic vesicle mobility in the synaptic vesicle cycle is still largely based on hypothetical assumptions, some of which have never been directly tested (see model in Fig. 1 A). Four stages can be defined: i), the synaptic vesicles are immobile at rest; ii), during stimulation vesicles move toward the plasma membrane and fuse with it; iii), after fusion the vesicle material diffuses laterally in the plasma membrane; and iv), the synaptic vesicle is endocytosed and actively moved back onto the vesicle cluster (note that the vesicle cluster is defined as an accumulation of vesicles, typically found in front of the active zones). Below, we present the current evidence regarding the different stages.

i. At rest, the synaptic vesicles are immobile. This hypothesis has been confirmed by numerous observations. For example, electron microscopy revealed vesicles that were tightly packed and interlinked (2), suggestive of low mobility. Vesicle clusters labeled via styryl (FM) dyes in preparations such as the frog neuromuscular junction (3) and hippocampal cultured neurons (4) were stable

in time. Movements were rarely detected (5) unless non-physiological treatments, such as incubation with the phosphatase inhibitor okadaic acid (6,7), were used. Fluorescence recovery after photobleaching (FRAP) studies confirmed the immobility of vesicles at rest (8), and further confirmation was provided by fluorescence correlation spectroscopy investigations (9–11).

ii. Movement of the vesicles toward the plasma membrane is still part of the current dogma regarding synaptic vesicle recycling, although no such movement has been observed in either conventional imaging of vesicle clusters labeled with FM dyes (12) or in FRAP studies (8). Moreover, one study in which only one vesicle was labeled per synapse and then tracked both at rest and during stimulation (13) indicated that movement was low in both cases.

iii. Movement of the fused vesicle material in the plasma membrane has never been directly investigated, mainly due to technical issues (for example, FM dyes are lost from the vesicles upon fusion). Some evidence was obtained from tagging synaptic proteins with pH-sensitive variants of GFP (pHluorins), which fluoresce only when the vesicles are fused to the plasma membrane (pHluorin molecules contained within the vesicles are quenched by the low pH of the vesicle). Movement of fused pHluorin-tagged proteins out of synapses and into the axons has been detected during prolonged high-frequency stimulation (14), but it is not clear whether this also happens under physiological stimulation, nor is it clear how the fused material moves (or whether it moves at all) under resting conditions.

iv. Movement of the vesicles back onto the vesicle cluster has never been imaged directly. One FRAP study in which vesicles were labeled with fluorescently labeled anti-synaptotagmin antibodies suggested that endocytosis may cause vesicle movement and fluorescence
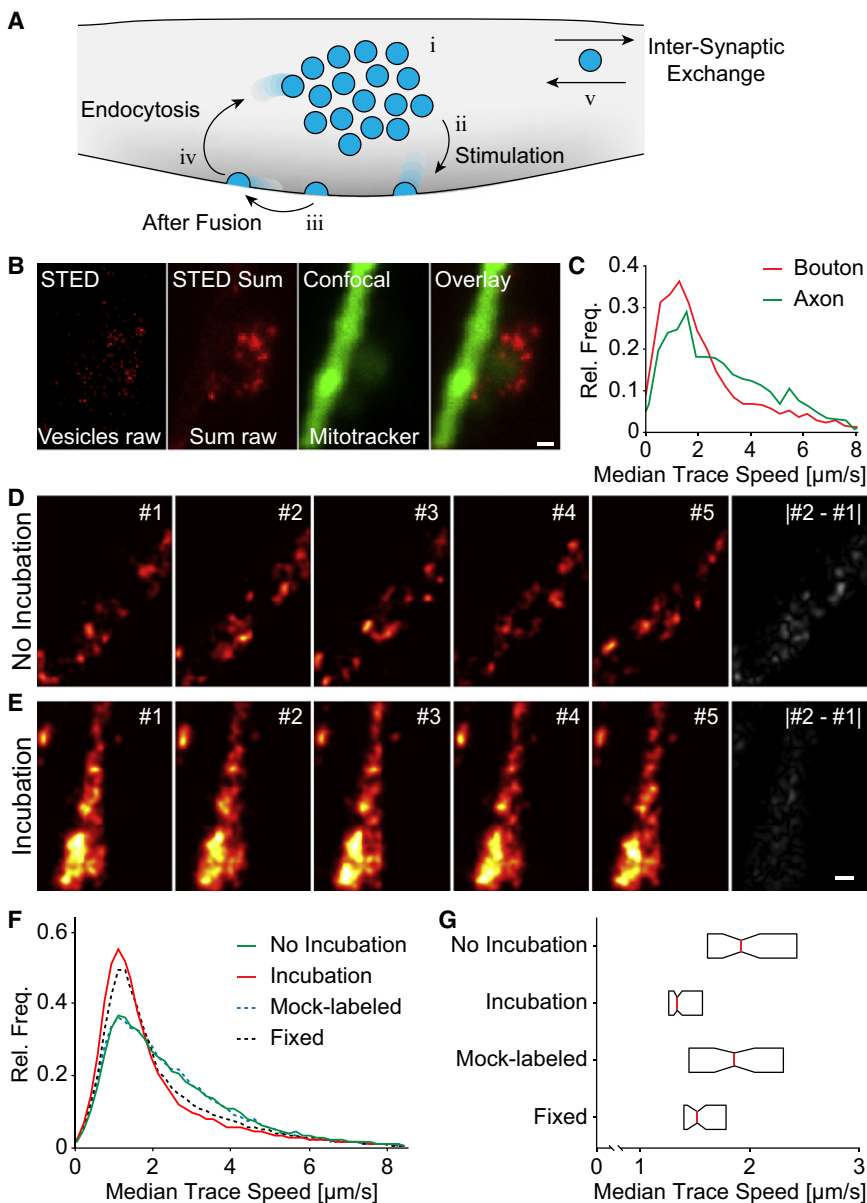
FIGURE 1 Mobility of synaptic vesicles is reduced after prolonged incubation. (*A*) Model of mobility in the vesicle cycle as commonly hypothesized in the literature. The vesicles are immobile at rest (i) and move toward the active zone upon stimulation (ii). Vesicle material may diffuse in the membrane after fusion (iii) before endocytosis brings the vesicle back into the cluster (iv). Vesicles may also move from one cluster to another in the axon (v). (*B*) Synaptic vesicle motion within an axon. Synaptic vesicles (shown in *red*) were labeled in cultured rat hippocampal neurons by anti-synaptotagmin monoclonal mouse antibodies. To give a clearer indication of the axon position, the mitochondria (shown in *green*) were also labeled by preincubation with 100 nM Mitotracker Green FM. The neurons were then imaged almost simultaneously in both the mitochondria (confocal) and synaptic vesicle (STED) channels (18 frames in the vesicle channel, followed by two frames in the mitochondria channel). Whereas individual STED frames taken at 28 frames/s show the instant location of the vesicles (*left panel*), summing all frames in the 22-s-long movie gives a good indication of the preferred moving areas (*second panel from left*). The brighter spots accumulate here around the smaller mitochondrial labeling site, at the side of the axonal mitochondrial tract, strongly suggesting that the area is a functional synaptic bouton. Scale bar: 250 nm; pixel size: 30×30 nm^2; dwell time: 3.7 μs at the center, increasing to the side. (*C*) Quantification of vesicle speed. The histograms show median trace speeds (median of the frame-to-frame speeds within one trace of a tracked vesicle) in the bouton-like and axonal areas. Note the higher speed in the axonal area, in accord with our previous findings (16). (*D* and *E*) Consecutive frames of a STED movie after digital filtering. These images show well-resolved synaptic vesicles stained against synaptotagmin and imaged within 5 min (*D*) or after 2 h of incubation (*E*). The gray panels show the difference images between the first and second frames. Scale bar: 250 nm; pixel size: 15×15 nm^2; dwell time: 0.93 μs at the center, increasing to the side. (*F*) Histogram of median trace speeds of synaptic vesicles in different conditions. Neurons imaged shortly after labeling are indicated in green. Neurons incubated at 37°C for 2 h before imaging are indicated in red. As a control, neurons mock-labeled (with buffer only), incubated for 2 h, and then labeled and imaged within 3–40 min are shown by the punctuated blue line. Aldehyde-fixed preparations are shown by the punctuated black line. For clarity, the error bars are not shown (see Fig. S1). Each histogram consists of 20,000–40,000 vesicle traces. (*G*) Boxplot of median trace speeds, showing the intersample variability. The red middle line gives the median (averaged over different samples) of the median trace speed within the different movies. The left and right ends of the boxes give the lower and higher quartiles, respectively. Boxes whose notches do not overlap have statistically different medians at a 5% significance level.

recovery (7), but no dynamic imaging was performed to analyze the potential movement.

Finally, one more step was recently added to the classic schema: intersynaptic vesicle exchange (v), which Darcy et al. (15) noted by photobleaching entire boutons and monitoring the fluorescence recovery. The relation of this observation to general vesicle recycling is not well understood, although it is generally thought that the movement along the axon must be faster than the movement within the synapse.

In an attempt to obtain a better understanding of the movement of synaptic vesicles, we recently introduced stimulated emission depletion (STED) microscopy to synaptic studies (16). In STED microscopy, a laser beam that excites fluorescent probes in the focal area is overlapped with a second, usually doughnut-shaped beam that switches off the fluorescence ability of the molecules. As a result, fluorescence originates only from the center of the excitation spot, where the intensity of this STED beam is close to zero. The effective focal volume generating the signal is thus much

narrower than the diffraction-limited excitation spot, leading to significantly higher resolution. Tracking multiple synaptic vesicles simultaneously allowed us to note that although many vesicles could be described as stable, many (or most) were mobile (16), in contradiction to the lack of mobility observed in the literature (see above). The vesicle mobility did not appear to change upon depolarization with K^+; however, since we were only able to investigate motion at a substantial time point after the addition of K^+ (minutes), we may have missed effects that were only visible at the onset or offset of stimulation.

To extend our initial observations and provide a thorough view of the multiple steps involved in synaptic vesicle recycling, we conducted a descriptive study of vesicle mobility. We found that only the recently endocytosed vesicles were mobile, whereas resting vesicles were essentially stable. Neither of these two pools showed a change in mobility upon physiological stimulation. Finally, an investigation of synaptic material fused onto the plasma membrane suggested that this material is surprisingly slow in its movement.

MATERIALS AND METHODS

Primary cultures and labeling

Primary cultures of neonatal rat hippocampal neurons were prepared as described previously (17). For labeling, the neurons were incubated for 5 min with anti-synaptotagmin monoclonal mouse antibodies (604.2) on ice (for selective surface staining), diluted in a Tyrode solution (17). They were briefly washed and incubated for 8 min with a dilution of Atto647N-labeled anti-mouse Fab fragments. The neurons were again washed, transferred to the microscope, and imaged in Tyrode solution for typically up to 30–40 min (No Incubation) or placed back in growth medium in a 37°C incubator for later imaging (Incubation). Incubated cells were taken out of the incubator, transferred to the microscope, and imaged in Tyrode solution at room temperature, again for up to 30–40 min. Mitochondrial labeling was performed by incubating the cultures with 100 nM Mitotracker Green FM at 37°C in growth medium. After 15 min the cultures were washed with Tyrode buffer and labeled with anti-synaptotagmin monoclonal mouse antibodies as described above. Fixed cells were prepared (after labeling) by incubation for 60 min with 3% glutaraldehyde and 2% paraformaldehyde. (Antibodies directly labeled against synaptotagmin can be used in the assay as well, although labeling with Atto647N generally compromises their ability to bind specifically. However, one recently obtained batch appears to be specific and was used in the experiment presented in Fig. 5.) Stimulation was performed using a platinum plate electrode (8 mm distance between the plates), and 100 mA shocks were delivered using an A310 Accupulser stimulator (World Precision Instruments, Berlin, Germany) at 20 Hz for 2 s.

Microscopy

Confocal fluorescence microscopy and FRAP were performed with a Leica TCS SP5 STED confocal microscope using a 100×, 1.4 numerical aperture HCX PL APO CS oil objective (Leica Microsystems, Mannheim, Germany). Excitation of Atto647N was achieved with a Helium-Neon laser at 633 nm, and fluorescence was detected in the spectral range of 641–750 nm. Immunohistochemistry was performed as previously described (17), with the exception that methanol fixation was used for GluR1 and synapsin. STED microscopy was performed as previously described (16) (see the Supporting Material for details).

STED data analysis

The positions of the vesicles were automatically determined in each frame as follows: all frames were first preprocessed to extract the areas containing vesicles. For this, we deconvolved each frame with a Gaussian function with a full width at half-maximum of 60–100 nm and a moderate quadratic potential regularization (18). This resulted in smooth images with unbroadened (undisturbed) structures. We then applied a low threshold, which eliminated background areas and delivered the areas in which the vesicles were contained. To determine the number of vesicles in each area, we divided the number of photons from each area by the average brightness of the vesicle (the average vesicle brightness, i.e., the mean number of photons detected from a single vesicle, was roughly determined by inspection of single vesicles in several movies). On average, each area above the threshold contained ~2 vesicles. We then performed a fit of the positions of the vesicles in the area. The fit modeled a variable number of vesicles (each with its own position and brightness) in the area, in the presence of modeled shot noise. To avoid overfitting (i.e., to avoid obtaining too many vesicles), we applied a penalty in the model, such that the modeled vesicles were not allowed to deviate strongly from the average vesicle brightness. We verified the strength of the penalty (the amount of deviation from the average vesicle brightness that was allowed by the fit) by manually inspecting the vesicle position/brightness produced by the fit in several movies. By collecting the data (vesicle number and positions) over all areas and frames, we obtained the final position map of localized vesicles for each movie. Some movies were evaluated with a faster algorithm, which yielded essentially the same results for the object localization. Raw images were first filtered by a 120 nm Gaussian. The locations of local maxima were taken as the object positions. Local maxima with intensities < 14% of the intensity of the brightest object in the image series were discarded. All localized objects were then tracked as described previously (16) (see the Supporting Material for details).

Confocal data analysis

All data analyses of the confocal and epifluorescence images were performed using routines written in MATLAB (The MathWorks, Natick, MA), as described in the Supporting Material.

RESULTS

STED microscopy demonstrates that recently endocytosed vesicles are mobile and the resting vesicles are largely stationary

In our previous study of synaptic vesicle movement (16), we identified a high level of vesicle motion at rest, which largely contradicted previous investigations (see Introduction). One experimental difference between our study (16) and most others is that we investigated vesicle motion shortly after endocytosis, i.e., we focused on the recently endocytosed pool of vesicles. Thus, it is possible that the recently endocytosed vesicles were more mobile than all other vesicles.

To investigate this, we labeled hippocampal cultures with monoclonal antibodies directed against the intravesicular domain of synaptotagmin. The antibodies were briefly applied to the neurons on ice (~2°C), which resulted in labeling of the synaptic vesicles that were fused to the plasma membrane (and therefore open to the outside space). To visualize the monoclonal antibodies, we then briefly incubated the cultures with anti-mouse Fab fragments coupled to

the dye Atto647N (see the Supporting Material for details). The labeling is specific for synaptic vesicles, which are rapidly endocytosed within 2–5 min after switching to room temperature (16). Imaging was performed with a STED setup (16,19) as described in the Supporting Material.

We first tested our previous observations that recently endocytosed vesicles are highly mobile (16). As shown in Movie S1, these vesicles are indeed mobile (see also Fig. 1 B). Moreover, by quantifying vesicle movement with single-particle-tracking procedures, we were able to demonstrate, as in our previous work, that movement is lower in synaptic areas than in the axon (Fig. 1 C). Therefore, these vesicles conform to some extent to the classical model, which holds that movement is slower in the synapse compared to the intersynaptic movement (which takes place in the axon), although the generally high rates of movement constitute a clear discrepancy.

To determine whether the high movement is characteristic of only the recently endocytosed pool, we incubated the preparations for 2 h (37°C) after labeling, a time period that is long enough to permit the functional mixing of recently endocytosed and resting vesicles (20). The movement was substantially lowered (Fig. 1, D and E, and Movie S2). The change in vesicle movement with incubation was all the more evident when difference images were generated between subsequent frames (*gray panels* in Fig. 1, D and E). Quantification of the vesicle speeds indicated that before incubation the vesicles were highly mobile, and after incubation their mobility was almost indistinguishable from that of aldehyde-fixed preparations (Fig. 1, F and G). The difference between the two vesicle mobility states is significant ($p = 2.5 \times 10^{-4}$, Wilcoxon's rank sum test; see also Fig. S1, where all curves are indicated with the corresponding error bars). As a control, we mock-labeled preparations, which is the same treatment used for normal labeling without the addition of antibodies, and incubated them for 2 h (37°C) before finally labeling them with anti-synaptotagmin antibodies as described above. The mobility of these vesicles was identical to that of control (nonincubated) preparations (Fig. 1, F and G), demonstrating that the labeling/incubation procedure does not affect general vesicle movement, and thus the observed difference is not a labeling artifact.

The decrease in motion is associated with integration within clusters

The immobilization of the vesicles can also be described by using a running average analysis of the movies (16). The areas in which vesicles move randomly appear as blurs, whereas the areas in which vesicles are stationary result in high-intensity or "hot" spots (16). The hot spots appear to be subunits of the vesicle clusters (the vesicle clusters contain several hot spots, as exemplified in Fig. 1 B). As
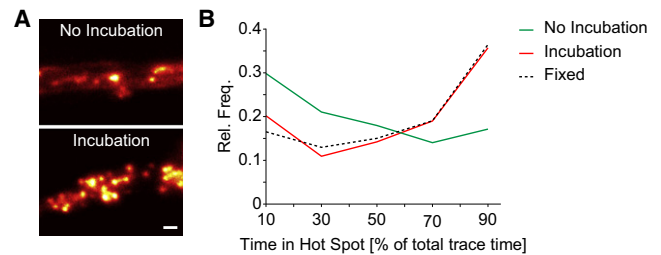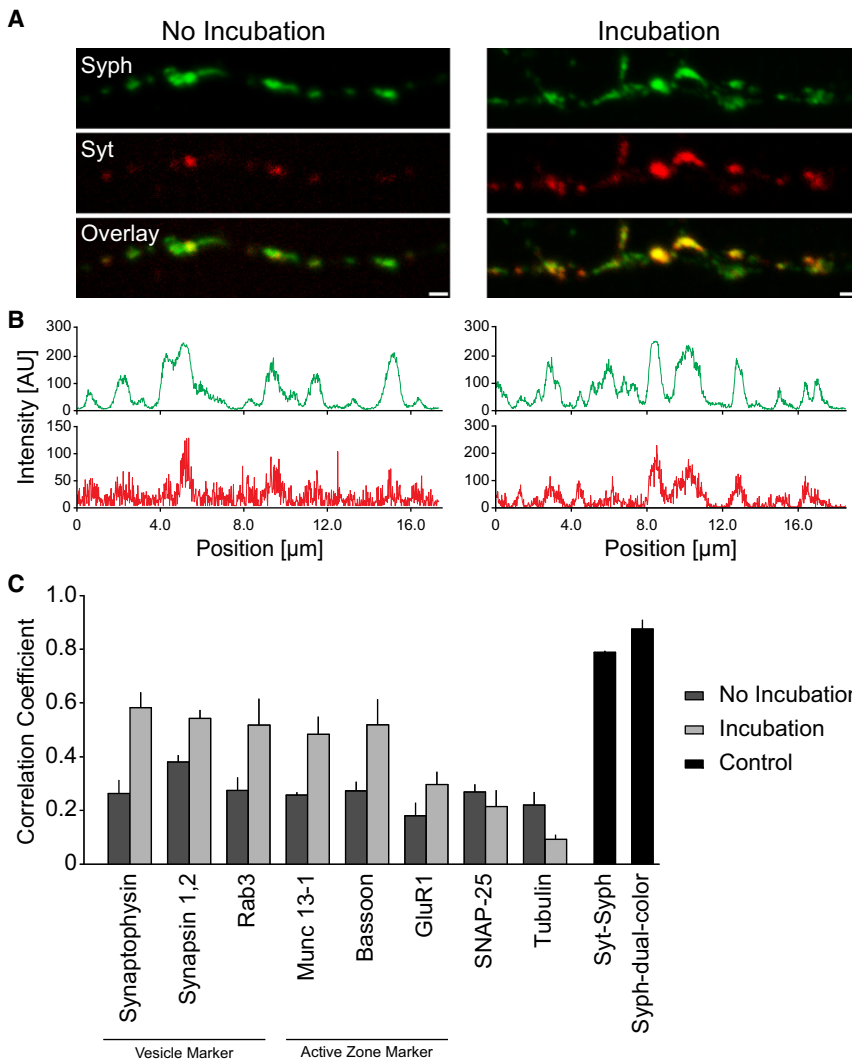

FIGURE 2 Stabilization of vesicles after incubation. (*A*) Preparations were either imaged shortly after endocytosis or incubated for 2 h at 37°C, and averaged images were obtained from the movies. Scale bar: 250 nm. (*B*) The time spent by each vesicle in hot spots was quantified as a fraction of the time the particular vesicle was tracked. The graphs show histograms from 1670–9850 tracks. Note that the incubated preparations are almost indistinguishable from aldehyde-fixed preparations.

indicated in our previous publication, the hot spots may be seen as pockets in the synaptic vesicle clusters where the vesicles are likely to bind and remain stationary (16). Therefore, a vesicle incorporated in a hot spot is automatically part of the vesicle cluster. We quantified the time spent by the vesicles in hot spots (Fig. 2, A and B) and found that it increases dramatically in incubated preparations, with the vesicles becoming essentially stationary, as in the aldehyde-fixed preparations.

To further analyze the location of the sequestered vesicles in vesicle clusters, we investigated the colocalization of the labeled vesicles with a number of synaptic markers, both before and after 37°C incubation. We labeled the cultures with antibodies against synaptotagmin as above (Fig. 3 A, *red*), and then fixed and permeabilized them. We subsequently immunostained the preparations for several general vesicle markers (synaptophysin, synapsin, and Rab3) and active zone markers (Munc 13, bassoon, or postsynaptic glutamate receptors (1)). Because the general vesicle markers are found on all vesicles, they serve as optimal markers for accumulations of vesicles (i.e., for the vesicle clusters as defined in the Introduction).

Typical images for synaptophysin are shown in Fig. 3 A (*green*). See Fig. S2 for typical images of all other markers (note also that the general appearance and fluorescence of the synaptotagmin-labeled axons does not change substantially during incubation, i.e., the vesicle marker is not lost upon incubation). A visual investigation suggests that the synaptotagmin-labeled vesicles show a higher degree of colocalization after incubation with both the general vesicle markers and active zone markers. This impression was confirmed by an investigation of the intensity line profiles through the axons (Fig. 3 B). The Pearson's correlation coefficient between the line profiles in the synaptotagmin and vesicle cluster/active zone marker channels (Fig. 3 C) increased after incubation for all immunostains. This suggests that the vesicles are loosely associated with the clusters after endocytosis, and integrate fully only after incubation. This hypothesis is confirmed by the finding that

A No Incubation / Incubation
Syph / Syt / Overlay

B Intensity [AU], Position [μm]

C Correlation Coefficient

FIGURE 3 Vesicle integration in clusters after incubation. (*A*) Colocalization of anti-synaptotagmin-labeled vesicles with synaptophysin. Neurons were stained as described against the lumenal domain of synaptotagmin (Syt, *red channel*), and fixed either after a 20-min rest period (*left panels*, No Incubation) or after 2 h of incubation (*right panels*, Incubation). They were then permeabilized and immunostained for the synaptic vesicle marker synaptophysin (Syph, *green channel*). Imaging was performed by confocal fluorescence microscopy. After incubation, a higher colocalization is visible in the overlay, although many synaptic boutons costain for the two markers in both conditions. Scale bar: 1 μm. Note that the fluorescence gain in the synaptophysin channel has been adjusted so that the vesicle clusters are not saturated; this implies that the signal from single vesicles is difficult to distinguish from background. Thus, the synaptophysin signal from synaptotagmin-positive vesicles found away from the clusters is hardly visible. (*B*) Line profiles of fluorescence intensity (in arbitrary units (AU)) of synaptophysin (*green*) and synaptotagmin (*red*) along the axons of the corresponding images in the left and right panels. Cross-correlation of these profiles was used for the analysis shown in *C*. (*C*) Correlation between live-stained synaptotagmin and immunostained neuronal markers. The preparations were stained using antibodies against synaptic vesicle markers (synaptophysin, synapsin, and Rab3), active zone-associated proteins (Munc 13 and bassoon), postsynaptic receptors (GluR1), membrane SNARE proteins (SNAP-25), and cytoskeletal elements (tubulin). Line profiles (as in *B*) were obtained and Pearson's correlation coefficients were calculated (No Incubation, *dark gray*; Incubation, *light gray*). The two right-most bars indicate positive controls for the correlation coefficient analysis: immunostaining of all vesicles for both synaptotagmin and syna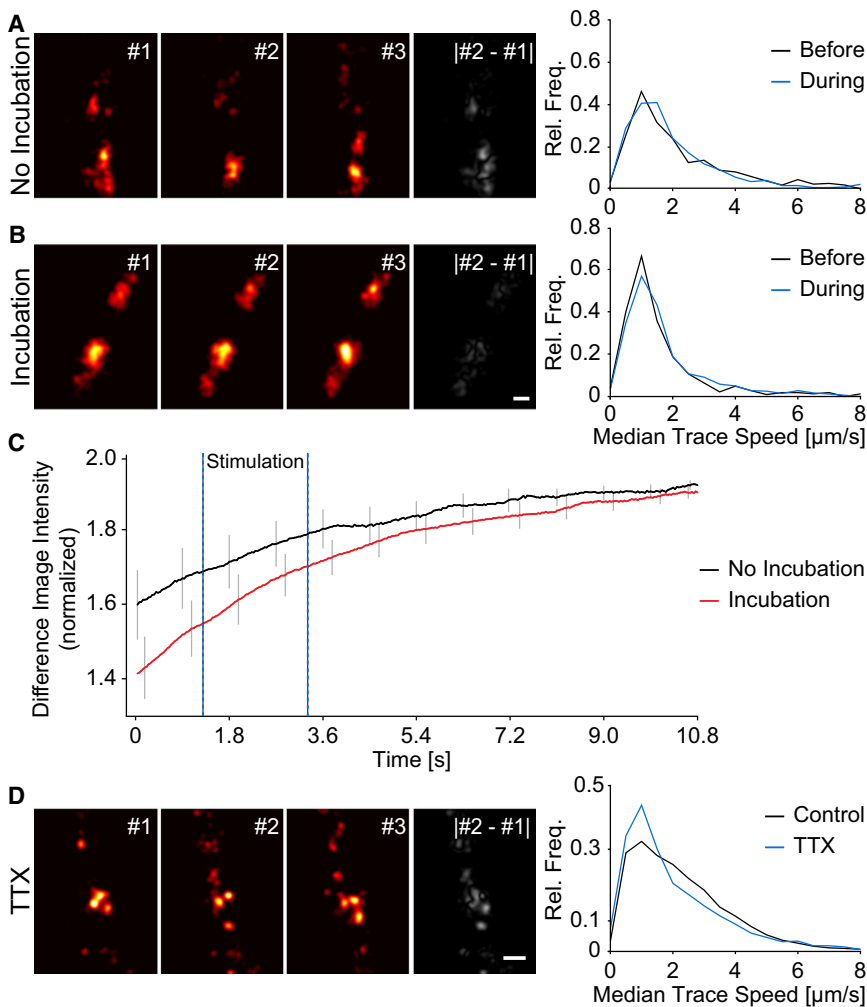ptophysin (Syt-Syph), or immunostaining for synaptophysin using a mixture of Cy3- and Cy5-labeled secondary antibodies (Syph-dual-color). The bars show the mean ± SE from at least three independent experiments for each condition. Typical colocalization patterns for all of the different immunostainings are shown in Fig. S2.

vesicle colocalization with tubulin decreases, in agreement with the fact that tubulin is more abundant in the axon than within the vesicle clusters (2). We found no change in the colocalization with a membrane protein whose localization is independent of the synaptic vesicle cluster location (SNAP-25 (21)), confirming the accuracy of our measurements.

These results suggest that synaptic vesicles undergo a change, or maturation process, that results in a strong decrease in mobility, and in their integration within preexisting vesicle clusters.

Of interest, the exchange of vesicles between synapses (the intersynaptic exchange) was similar for both the incubated and nonincubated preparations (for both recently endocytosed and resting vesicles). This observation, based on FRAP imaging of the different conditions (Fig. S3), suggests that basic vesicle mobility and intersynaptic exchange (22) are governed by different mechanisms.

Electrical stimulation has no detectable effects on vesicle mobility

Arguably, the most important event in a synaptic vesicle's lifetime is exocytosis. However, as indicated in the Introduction, it is still unclear what the effects of stimulation are, because although the hypothetical model suggests that motion should take place upon stimulation, no such motion has yet been observed. Moreover, it is difficult to predict how stimulation will affect different (recently endocytosed versus resting) vesicles.

We analyzed synaptic vesicles before and during stimulation. We restricted our investigation to a short, high-intensity stimulation procedure (20 Hz for 2 s) that is known to cause recycling of the readily releasable pool of synaptic vesicles (23). In a previous study using this procedure (24), we observed that ~19% of the vesicles were recycled (note also that ~50% of the vesicles are nonreleasable in this

FIGURE 4 Effects of electrical stimulation on vesicle mobility. (*A* and *B*) Left panels show a series of frames during stimulation for nonincubated (*A*) and incubated (*B*) preparations. Gray panels show the difference images between the first and second frames. Scale bar: 250 nm. Graphs show the histograms of median trace speeds. Values during stimulation are shown in blue, and values in the absence of stimulation are shown in black. Each histogram contains 550–730 values. (*C*) Analysis of vesicle mobility independent of tracking. The intensity in difference images was calculated for each (raw data) frame of the movie, normalized to the frame's intensity. As the frames become dimmer with bleaching, the difference images tend to appear proportionally brighter (hence the upward trend in the curves). The plots were smoothed by applying a 15-frame moving average. The graphs show the mean $\pm$ SE from 20 (No incubation) and 51 (Incubation) movies. Note that no substantial change in this measurement appears at the onset/end of stimulation (indicated by *dotted lines*). (*D*) Neurons were labeled against synaptotagmin and were then incubated with tetrodotoxin (TTX, 1 μM) for 10 min at room temperature. The series of panels shows three frames of a typical movie. The gray panel shows the difference image between the first and second frames. Scale bar: 250 nm. The graph shows a histogram of median trace speeds for the TTX incubation (2490 values, *blue*) compared with the control condition (without tetrodotoxin, *black*).

preparation). Stimulation did not seem to affect the mobility of either the recently endocytosed vesicles or the resting ones (see also Movie S3), and vesicle tracking indicated no substantial increase (or decrease) in motion during stimulation (Fig. 4, *A* and *B*). As a second, independent measure of vesicle movement, we calculated the difference images between subsequent frames of the movies for both the recently endocytosed and resting vesicles. The intensity in the difference images (after normalization to the intensity of the movie frames) is a direct measure of mobility, as stable vesicles report substantially smaller differences from one frame to the next (see *gray panels* in Fig. 4, *A* and *B*). No change in the difference image intensity was observed upon the onset or end of stimulation, suggesting that stimulation leaves most vesicles unaffected (Fig. 4 *C*).

To investigate the converse process, i.e., whether inhibiting synaptic activity affects motion, we incubated the preparations with tetrodotoxin (TTX, 1 μM) for 10 min after labeling (Fig. 4 *D*, Movie S4). Of interest, a decrease in motion was observed (Fig. 4 *D*). Thus, the recently endocytosed vesicles may switch more rapidly toward the cluster

integration pathway under conditions of inactivity; in other words, activity may keep the mobile vesicles in motion.

Mobility of synaptic vesicle material on the plasma membrane

After exocytosis, the synaptic vesicle material finds itself in the plasma membrane. This process is not easy to image, because the vesicles are endocytosed relatively rapidly (16). However, since endocytosis is calcium-dependent, it can be inhibited by a reduction in the concentration of divalent ions (25,26). This allows the investigation of a small amount of vesicle material that remains on the surface and corresponds to the fused vesicles found at equilibrium. To increase the number of fused vesicles (through stimulation), vesicle fusion must be induced by a means that is independent of depolarization (i.e., independent of calcium entry into the nerve terminals, which in turn would also trigger endocytosis). One possible approach is to use black widow spider venom (BWSV) (27), which causes synaptic release in a calcium-independent fashion. A second possibility is
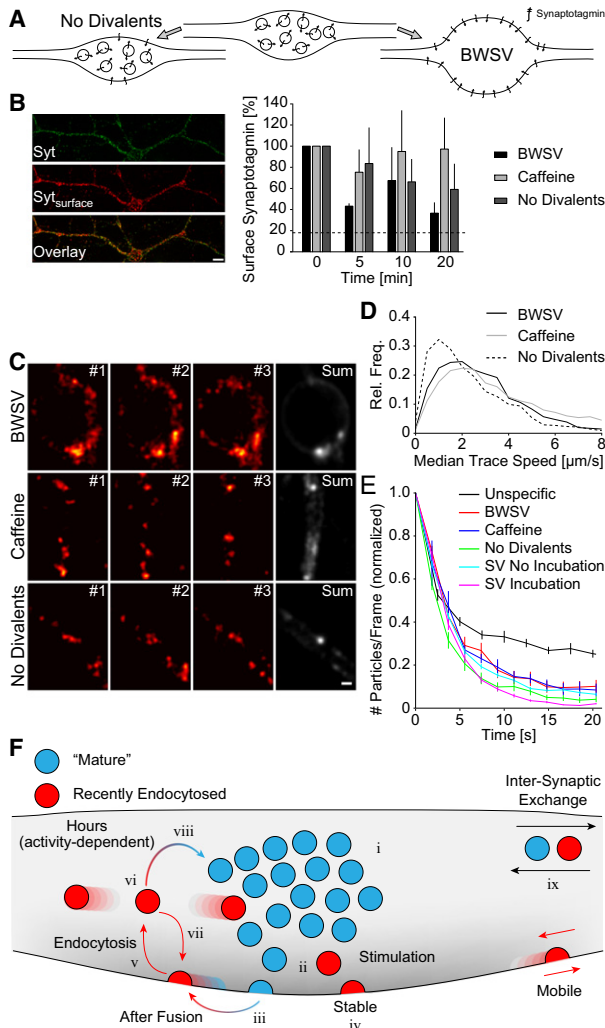
FIGURE 5 Mobility of fused synaptic vesicle material. (*A*) Experimental schematic. Inhibiting endocytosis by removing divalent ions allows specific imaging of the surface pool of synaptotagmin (*left*). Additional stimulation (via BWSV or caffeine) increases this pool (*right*); note that the increase in stimulation induced by BWSV is larger than that induced by caffeine. (*B*) Quantification of the surface pool of synaptotagmin. Preparations were incubated with BWSV or caffeine, or placed in divalent-free Tyrode before surface staining with an Oyster-550-labeled anti-synaptotagmin antibody (*green*). At different time points after staining, we fixed the preparations and labeled the antibodies remaining on the surface using a Cy5-coupled secondary antibody (*red*). Scale bar: 5 μm. The relative amount of antibody on the surface was determined and expressed as a percentage of the control condition (fixed immediately after labeling). The bars show the mean $\pm$ SE from three independent experiments for each condition. The dotted line indicates the amount of synaptotagmin left exposed in control conditions after only 2 min of incubation (16). Note that for all time points considered, all three conditions allow a large fraction of synaptotagmin molecules to remain on the surface instead of being endocytosed, with the effect being strongest in the case of caffeine treatment. (*C*) Movement of synaptotagmin on the plasma membrane. Neuronal cultures were incubated with BWSV or caffeine, or placed in divalent-free Tyrode buffer before labeling and imaging (as above). Three consecutive frames are shown for each condition (*top*, BWSV; *middle*, caffeine; *bottom*, no divalents). The gray panels show summed movie images, obtained by summing 500 frames. Note the presence of several bright spots, indicative of preferred areas (where the fluorescent material remained relatively stationary). Scale bar: 250 nm. (*D*) Histograms

to use caffeine in the absence of extracellular divalents, which stimulates the release of a limited amount of calcium from intracellular stores, sufficient for exocytosis; the subsequent endocytosis is nevertheless inhibited (26). We found that the caffeine and BWSV treatments increased exocytosis by ~32% and ~60%, respectively, as observed by quantifying the amount of synaptotagmin on the surface membrane ($n = 3$ independent experiments; increases were significant, $p < 0.05$, t-test).

We used these different protocols to investigate the mobility of fused vesicle material (Fig. 5 *A*). Endocytosis was severely inhibited in all three cases, as observed by quantifying the amount of vesicle material remaining on the plasma membrane at different time points after labeling (Fig. 5 *B*). The movement of fused components is presented in Fig. 5 *C* (see also Movie S5). Tracking suggested that the surface pool is mobile under normal (unstimulated) conditions, and that the mobility increases after stimulation via either BWSV or caffeine (Fig. 5 *D*). This suggests that under normal conditions, the surface fraction of vesicle material is kept at a (relatively) low mobility, perhaps in the form of clathrin-coated pits (see below). The fused material escapes the mechanisms that limit mobility when its quantity is increased by stimulation.

When the movement of fused synaptic vesicle components was monitored over time, the signal bleached relatively rapidly, with little fluorescence entering the imaged area after ~15 s (Fig. 5 *E*). When a nonspecific antibody (a clone 604.2 antibody against synaptotagmin, directly labeled with Atto647N, which completely lost specificity due to the labeling; Fig. S4) was used, the entry of labeled antibodies in the imaged area was observable for much longer. The fraction of particles that persisted at equilibrium in the imaged area, maintained through constant entry of labeled antibodies, was 26% $\pm$ 1% (mean $\pm$ SE) for the nonspecific labeling, which is substantially higher than the 4.1% obtained for surface-stained nerve terminals (Fig. 5 *E*, no

of median trace speeds. Note the higher mobility for caffeine and BWSV. Each histogram contains 2500–3000 values. (*E*) Motion analysis by bleaching. We quantified the amount of fluorescent particles per 50 movie frames, expressed as a fraction of the particle number in the initial 50 frames. The SE is derived from different movies. With bleaching, the number of particles decreases rapidly for both surface staining and internalized vesicles. In contrast, fluorescence persists at a much higher level in a preparation stained with an antibody that binds nonspecifically to the membrane (and is therefore presumably not limited in its movement), as unbleached dye constantly enters the field of view. SV = synaptic vesicles (in contrast to surface staining, as shown in all other traces). (*F*) Model of vesicle motion. Resting, mature vesicles are immobile (*blue*, i). Vesicle mobility does not change upon stimulation (ii). Vesicle material may move after fusion (iii), but a substantial fraction has low mobility (iv). Endocytosis (v) generates the recently endocytosed mobile vesicles (*red*, vi). Repeated recycling keeps these vesicles in the mobile pool (vii), but eventually they integrate into the resting vesicle cluster (viii). Both the resting and recently endocytosed vesicles move between clusters/synapses (ix).

divalents) or the 8.6% and 9.8% obtained for the caffeine and BWSV treatments.

To investigate the potential sequestering mechanisms that keep the motion of fused vesicles to a relatively low level, we immunostained the cultures (as in Fig. 2) with antibodies against clathrin or amphiphysin (Fig. S5 A). A significant ($p < 0.01$, t-test) correlation between the fused synaptic vesicle material and these endocytosis markers was found (Fig. S5 B), suggesting that some of the fused vesicles may already be in the form of clathrin-coated pits.

DISCUSSION

In this work, we generated a model of vesicle mobility (Fig. 5 F) that is substantially more complex than the classic one (cf. Fig. 1 A). Resting vesicles (*blue*) are immobile (i), as proposed previously. Stimulation, in contrast to the previous hypothesis, does not result in any change in motion (ii). After fusion, the vesicle material may move away (iii), but a substantial fraction has only low mobility (iv). The endocytosis process (v) results in the appearance of recently endocytosed mobile vesicles (*red*, vi). These vesicles may fuse again and thus remain in the mobile pool (vii), but they eventually lose their mobility and integrate into the resting vesicle cluster (viii). Both the resting and recently endocytosed vesicles are exchanged between synapses (ix). Our results, obtained by labeling vesicles with antibodies, are in agreement with findings derived from other techniques such as styryl (FM) dye labeling (which would be expected, since the two approaches stain the same vesicles (5,7)), which showed that vesicles move between and within synapses (9,13,15), exchange between synapses (15), and may also appear fairly immobile within synapses (9,13).

We discuss the implications of the different steps below.

The finding that the resting vesicles are immobile (i) reconciles our previous observations (16) with the numerous low-mobility values reported in the literature. The physiological role of this inert resting pool is likely limited, since the organelles forming the part of the cluster away from the active zone would rarely fuse. However, it is possible that the resting vesicles found at the active zone would fuse upon stimulation and therefore become active vesicles (note that a substantial fraction of these vesicles can fuse upon tetanic, unphysiological stimulation, for example (29)). It has been shown that in the frog neuromuscular junction, the reserve pool is also immobile, unlike the recycling vesicles (30); however, it is possible that most reserve vesicles are less releasable in hippocampal cultured synapses than in neuromuscular preparations, which may be one reason for their immobility.

Stimulation (ii) results in no changes in vesicle motion. Our results provide a simple explanation for this puzzling observation: First, the mobile vesicles are already mobile enough to reach the active zones, and therefore stimulation only changes their ability to fuse, not their movement.

Second, the resting vesicles that already find themselves docked at the active zones will simply collapse into the membrane, without an increase in mobility. This interpretation is in agreement with the fact that many more vesicles are docked at active zones than are likely to fuse upon a few action potentials, possibly representing docked resting vesicles that fuse only occasionally. In a quantitative study, Schikorski and Stevens (23) indicated that 10–20 vesicles are docked at active zones in our preparations, whereas one action potential generally releases less than one vesicle (31). Of interest, inhibiting synaptic activity by the addition of TTX slowed the movement of recently endocytosed vesicles. To our knowledge, our observation that synaptic silencing decreases vesicle mobility provides the first correlation between vesicle motion and synapse activity. This observation is in agreement with the synapsin hypothesis of vesicle movement (32), which states that the synapsin molecules bind to both actin and synaptic vesicles, thereby fixing and cross-linking the clustered vesicles. Upon stimulation and calcium entry into the nerve terminals, synapsin is phosphorylated and unbinds from the vesicles, which would increase their motion. A cessation of activity would decrease calcium entry and synapsin phosphorylation, and would thus trigger a stronger cross-linking of the vesicles (note, however, that the role of synapsin in vesicle movement is still under scrutiny (33)).

It has been proposed that the vesicle molecules diffuse widely out of the synapses after exocytosis (iii and iv), and the vesicle structure is therefore lost upon fusion (14,34,35). We found, surprisingly, that the motion of fused vesicle components is no higher than that of recently endocytosed vesicles, at least under normal conditions (in the absence of additional stimulation). This observation is in agreement with our recent finding that synaptotagmin molecules are found on the plasma membrane in multimolecular clusters that likely represent fused vesicles (17) and may contain not only synaptotagmin but also other vesicle components (36). A number of arguments can be made in favor of this interpretation. First, the presence of several of the labeled molecules in stable (low-mobility) spots argues against a free-diffusion model (which would be expected for single molecules). Second, their (weak) association with clathrin points in the direction of multimolecular aggregates. Third, a free-diffusion model would predict that free molecules would constantly enter the imaged area, which was not the case (few vesicle components entered after ~15–20 s of imaging). Altogether, our observations suggest that after fusion, the vesicle material does not disaggregate into widely diffusing components; rather, it remains as patches of relatively low mobility that are then targeted by the clathrin machinery. The pits are unlikely to have progressed far beyond the initial coating stages, since almost no endocytic vesicle openings (Ω figures) can be found without stimulation (37,38), and thus may be partly assembled synaptic vesicle material/clathrin machinery aggregates.

The advantage of having low-mobility clathrin-coated pits in the boutons has been indicated by the experiments of Gandhi and Stevens (31), who noted that upon stimulation, vesicles could be rapidly endocytosed. This would be possible only if the vesicle material were stably maintained at an endocytosis site from which it could be retrieved. The increase in mobility after BWSV or caffeine treatments likely results from some of the newly fused material being outside of the clathrin-coated pits, since it is known that some vesicles may escape the clathrin mechanisms even after substantial stimulation (39).

In perhaps our most important observation, we found that endocytosis (v) results in the formation of a class of vesicles–the mobile, recently endocytosed vesicles (vi)—that are widely different from the resting ones. This finding is in agreement with a FRAP study at the frog neuromuscular junction, which indicated that the recycling pool is more mobile than the so-called reserve pool (30). However, this is the first time, to our knowledge, that a change in vesicle behavior has been noted after endocytosis. Virtually all models of synaptic vesicle recycling predict that a perfect vesicle will result after endocytosis (1), a process that would take at most a few minutes. Our results indicate that the vesicles remain mobile for substantial amounts of time (tens of minutes at room temperature) before integrating into vesicle clusters. The importance of this mobility can only be surmised; it would certainly allow these vesicles to arrive at the active zones and eventually fuse again (vii), but many other models of directed motion would serve this purpose much better.

The molecular changes underlying the change from the mobile to the resting state (viii) are difficult to pinpoint at present. However, one suggestion is provided by the fact that inactivity speeds the process, and, conversely, the mobile vesicles escape cluster integration (and the loss of mobility) by repeated recycling. It has been shown that fused vesicles do not contain synapsin (40), the molecule that is the most likely candidate for enabling the cross-linking of synaptic vesicles (see above). Therefore, we speculate that the vesicles lose synapsin during or after exocytosis, with the recently endocytosed vesicles becoming free of it and therefore mobile. As long as these vesicles remain synapsin-free, or bind only a limited number of synapsin molecules (note that an average vesicle contains ~8 synapsin molecules (41)), they will continue to be mobile. They eventually will bind more synapsin molecules (as suggested by Bloom et al. (40)) and become less mobile as the synapsin cross-links them to other vesicles and forces them onto hot spots in the vesicle clusters. We tentatively describe this process as the maturation of a mobile vesicle into a cluster-integrated one.

We conclude that the mobility of the synaptic vesicle changes during the recycling process, with the most striking difference being between the immobile resting vesicles and the highly mobile, recently endocytosed vesicles.

SUPPORTING MATERIAL

REFERENCES

1. Südhof, T. C. 2004. The synaptic vesicle cycle. *Annu. Rev. Neurosci.* 27:509–547.

2. Hirokawa, N., K. Sobue, …, H. Yorifuji. 1989. The cytoskeletal architecture of the presynaptic terminal and molecular structure of synapsin 1. *J. Cell Biol.* 108:111–126.

3. Betz, W. J., and G. S. Bewick. 1992. Optical analysis of synaptic vesicle recycling at the frog neuromuscular junction. *Science.* 255:200–203.

4. Ryan, T. A., H. Reuter, …, S. J. Smith. 1993. The kinetics of synaptic vesicle recycling measured at single presynaptic boutons. *Neuron.* 11:713–724.

5. Kraszewski, K., O. Mundigl, …, P. De Camilli. 1995. Synaptic vesicle dynamics in living cultured hippocampal neurons visualized with CY3-conjugated antibodies directed against the lumenal domain of synaptotagmin. *J. Neurosci.* 15:4328–4342.

6. Betz, W. J., and A. W. Henkel. 1994. Okadaic acid disrupts clusters of synaptic vesicles in frog motor nerve terminals. *J. Cell Biol.* 124:843–854.

7. Kraszewski, K., L. Daniell, …, P. De Camilli. 1996. Mobility of synaptic vesicles in nerve endings monitored by recovery from photobleaching of synaptic vesicle-associated fluorescence. *J. Neurosci.* 16:5905–5913.

8. Henkel, A. W., L. L. Simpson, …, W. J. Betz. 1996. Synaptic vesicle movements monitored by fluorescence recovery after photobleaching in nerve terminals stained with FM1-43. *J. Neurosci.* 16:3960–3967.

9. Jordan, R., E. A. Lemke, and J. Klingauf. 2005. Visualization of synaptic vesicle movement in intact synaptic boutons using fluorescence fluctuation spectroscopy. *Biophys. J.* 89:2091–2102.

10. Shtrahman, M., C. Yeung, …, X. L. Wu. 2005. Probing vesicle dynamics in single hippocampal synapses. *Biophys. J.* 89:3615–3627.

11. Yeung, C., M. Shtrahman, and X. L. Wu. 2007. Stick-and-diffuse and caged diffusion: a comparison of two models of synaptic vesicle dynamics. *Biophys. J.* 92:2271–2280.

12. Betz, W. J., G. S. Bewick, and R. M. Ridge. 1992. Intracellular movements of fluorescently labeled synaptic vesicles in frog motor nerve terminals during nerve stimulation. *Neuron.* 9:805–813.

13. Lemke, E. A., and J. Klingauf. 2005. Single synaptic vesicle tracking in individual hippocampal boutons at rest and during synaptic activity. *J. Neurosci.* 25:11034–11044.

14. Sankaranarayanan, S., and T. A. Ryan. 2000. Real-time measurements of vesicle-SNARE recycling in synapses of the central nervous system. *Nat. Cell Biol.* 2:197–204.

15. Darcy, K. J., K. Staras, …, Y. Goda. 2006. Constitutive sharing of recycling synaptic vesicles between presynaptic boutons. *Nat. Neurosci.* 9:315–321.

16. Westphal, V., S. O. Rizzoli, …, S. W. Hell. 2008. Video-rate far-field optical nanoscopy dissects synaptic vesicle movement. *Science*. 320:246–249.

17. Willig, K. I., S. O. Rizzoli, …, S. W. Hell. 2006. STED microscopy reveals that synaptotagmin remains clustered after synaptic vesicle exocytosis. *Nature*. 440:935–939.

18. Vicidomini, G., P. Boccacci, …, M. Bertero. 2009. Application of the split-gradient method to 3D image deconvolution in fluorescence microscopy. *J. Microsc.* 234:47–61.

19. Westphal, V., M. A. Lauterbach, …, S. W. Hell. 2007. Dynamic far-field fluorescence nanoscopy. *N. J. Phys.* 9:435.

20. Pyle, J. L., E. T. Kavalali, …, R. W. Tsien. 2000. Rapid reuse of readily releasable pool vesicles at hippocampal synapses. *Neuron*. 28:221–231.

21. Punge, A., S. O. Rizzoli, …, S. W. Hell. 2008. 3D reconstruction of high-resolution STED microscope images. *Microsc. Res. Tech.* 71:644–650.

22. Staras, K. 2007. Share and share alike: trading of presynaptic elements between central synapses. *Trends Neurosci.* 30:292–298.

23. Schikorski, T., and C. F. Stevens. 2001. Morphological correlates of functionally defined synaptic vesicle populations. *Nat. Neurosci.* 4:391–395.

24. Opazo, F., A. Punge, …, S. O. Rizzoli. 2010. Limited intermixing of synaptic vesicle components upon vesicle recycling. *Traffic*. 11:800–812.

25. Cousin, M. A., and P. J. Robinson. 2001. The dephosphins: dephosphorylation by calcineurin triggers synaptic vesicle endocytosis. *Trends Neurosci.* 24:659–665.

26. Zefirov, A. L., M. M. Abdrakhmanov, …, P. N. Grigoryev. 2006. The role of extracellular calcium in exo- and endocytosis of synaptic vesicles at the frog motor nerve terminals. *Neuroscience*. 143:905–910.

27. Henkel, A. W., and W. J. Betz. 1995. Monitoring of black widow spider venom (BWSV) induced exo- and endocytosis in living frog motor nerve terminals with FM1-43. *Neuropharmacology*. 34:1397–1406.

28. Reference deleted in proof.

29. Rizzoli, S. O., and W. J. Betz. 2004. The structural organization of the readily releasable pool of synaptic vesicles. *Science*. 303:2037–2039.

30. Gaffield, M. A., S. O. Rizzoli, and W. J. Betz. 2006. Mobility of synaptic vesicles in different pools in resting and stimulated frog motor nerve terminals. *Neuron*. 51:317–325.

31. Gandhi, S. P., and C. F. Stevens. 2003. Three modes of synaptic vesicular recycling revealed by single-vesicle imaging. *Nature*. 423:607–613.

32. Hilfiker, S., V. A. Pieribone, …, P. Greengard. 1999. Synapsins as regulators of neurotransmitter release. *Philos. Trans. R. Soc. Lond. B Biol. Sci.* 354:269–279.

33. Gaffield, M. A., and W. J. Betz. 2007. Synaptic vesicle mobility in mouse motor nerve terminals with and without synapsin. *J. Neurosci.* 27:13691–13700.

34. Wienisch, M., and J. Klingauf. 2006. Vesicular proteins exocytosed and subsequently retrieved by compensatory endocytosis are nonidentical. *Nat. Neurosci.* 9:1019–1027.

35. Fernández-Alfonso, T., R. Kwan, and T. A. Ryan. 2006. Synaptic vesicles interchange their membrane proteins with a large surface reservoir during recycling. *Neuron*. 51:179–186.

36. Bennett, M. K., N. Calakos, …, R. H. Scheller. 1992. Synaptic vesicle membrane proteins interact to form a multimeric complex. *J. Cell Biol.* 116:761–775.

37. Heuser, J. E., and T. S. Reese. 1981. Structural changes after transmitter release at the frog neuromuscular junction. *J. Cell Biol.* 88:564–580.

38. Heuser, J. E., T. S. Reese, …, L. Evans. 1979. Synaptic vesicle exocytosis captured by quick freezing and correlated with quantal transmitter release. *J. Cell Biol.* 81:275–300.

39. Miller, T. M., and J. E. Heuser. 1984. Endocytosis of synaptic vesicle membrane at the frog neuromuscular junction. *J. Cell Biol.* 98:685–698.

40. Bloom, O., E. Evergren, …, O. Shupliakov. 2003. Colocalization of synapsin and actin during synaptic vesicle recycling. *J. Cell Biol.* 161:737–747.

41. Takamori, S., M. Holt, …, R. Jahn. 2006. Molecular anatomy of a trafficking organelle. *Cell*. 127:831–846.